

Article

# 2D Enantioselective Disposable Stochastic Sensor for Fast Real-Time Enantioanalysis of Glutamine in Biological Samples

Raluca-Ioana Stefan-van Staden <sup>1,2,\*</sup> , Mihaela Iuliana Boga <sup>1,2</sup>, Ruxandra-Maria Ilie-Mihai <sup>1,\*</sup> ,  
Damaris-Cristina Gheorghe <sup>1</sup>  and Marius Badulescu <sup>3</sup>

- <sup>1</sup> Laboratory of Electrochemistry and PATLAB, National Institute of Research for Electrochemistry and Condensed Matter, 202 Splaiul Independentei Str., 060021 Bucharest, Romania
- <sup>2</sup> Faculty of Chemical Engineering and Biotechnologies, Politehnica University of Bucharest, 011061 Bucharest, Romania
- <sup>3</sup> Low Temperature Plasma Laboratory, National Institute for Lasers, Plasma and Radiation Physics (NILPRP), 409 Atomistilor St., 077125 Magurele, Romania
- \* Correspondence: ralucaivanstaden@gmail.com (R.-I.S.-v.S.); i.ruxandra04@yahoo.com (R.-M.I.-M.); Tel.: +40-751507779 (R.-I.S.-v.S.)

**Abstract:** As protein is both a structural component and a metabolic intermediary, amino acids play a crucial function in the body. When it comes to proteins, only the L-configuration of chiral amino acids is found. At the molecular level, symmetry is disrupted; however, the scientific basis for this symmetry breaking is not yet known. Enantioanalysis of chiral compounds such as amino acids plays a very important role in the correct diagnosis of illnesses, such as cancer. The enantiomers of glutamine—a chiral amino acid—were investigated in biological samples using a disposable stochastic sensor. The disposable stochastic sensor based on immobilization of maltodextrin (DE 4.0–7.0) on the surface of a disposable sensor based on graphene decorated with Ag was designed, characterized, and validated for screening tests of whole blood and tissue samples. The stochastic sensor was designed using cold plasma deposition of graphene decorated with Ag on plastic material. The sensor was enantioselective, being able to discriminate between the enantiomers of glutamine. High sensitivities were recorded for both enantiomers, while the limits of determination were 100 fmol L<sup>-1</sup> for L-glutamine and 1 fmol L<sup>-1</sup> for D-glutamine. High recoveries were determined for the assay of one enantiomer in the presence of the other, despite the ratio between the two enantiomers.

**Keywords:** Glutamine; enantioanalysis; disposable stochastic sensor; gastric cancer



**Citation:** Stefan-van Staden, R.-I.; Boga, M.I.; Ilie-Mihai, R.-M.; Gheorghe, D.-C.; Badulescu, M. 2D Enantioselective Disposable Stochastic Sensor for Fast Real-Time Enantioanalysis of Glutamine in Biological Samples. *Symmetry* **2023**, *15*, 958. <https://doi.org/10.3390/sym15050958>

Academic Editor: Miroslav Miletin

Received: 6 February 2023

Revised: 17 April 2023

Accepted: 20 April 2023

Published: 22 April 2023



**Copyright:** © 2023 by the authors. Licensee MDPI, Basel, Switzerland. This article is an open access article distributed under the terms and conditions of the Creative Commons Attribution (CC BY) license (<https://creativecommons.org/licenses/by/4.0/>).

## 1. Introduction

Stomach cancer is the fourth most fundamental sickness and the second leading cause of death on the planet. Because of the way that most patients present with advanced symptoms, it remains hard to heal effectively. Along these lines, how to identify early gastric cells is a remarkable test for early investigation and treatment of patients with gastric cancer development. Numerous studies on glutamine metabolism in cancer indicate that many tumors are avid glutamine consumers in vivo and in vitro.

Furthermore, an increasing amount of evidence indicates that the regulation of glutamine metabolism is influenced by various factors, such as the origin of the tumor, the status of oncogenes/tumor suppressors, epigenetic modifications, and the microenvironment of the tumor [1,2]. Notwithstanding the developing comprehension of the rationale behind the reliance of cancer cells on glutamine for their growth and survival, the role of glutamine metabolism in the advancement of tumors in physiological settings is still being explored. This is partly due to the fact that the concentration of glutamine in the tumor microenvironment is frequently observed to be low [2]. Given that targeting the acquisition and utilization of glutamine has been suggested as a novel therapeutic approach in cancer treatment, it is imperative to comprehend how tumor cells react and adjust to glutamine

deprivation in order to optimize therapeutic intervention. Growing data in recent years has confirmed that glutamine, commonly known as Gln, is an essential metabolic substrate and a source of life for certain tumor cells. “Glutamine dependence” is exhibited by these tumor cells, which need Gln to survive and continue growing [3,4]. In any case, researchers have only just become aware of the complex metabolic reasoning behind the growing cancer cells’ dependence on Gln, which goes much beyond the satisfaction of dynamic and biosynthetic demands.

Throughout the chemotherapy regimen, encompassing the recuperative phase, a notable reduction in glutamine levels was observed among tumor patients in comparison to the control cohort. Moreover, the concentrations of glutamine exhibited a nearly four-fold reduction as compared to the prechemotherapy phase [4]. The notable reduction in glutamine concentrations can be ascribed to multiple factors, including diminished appetite resulting from capecitabine, insufficient ingestion or absorption of crucial amino acids, and inadequate utilization of all amino acids. Studies have indicated that Glutamine may have the potential to enhance digestive function, augment lymphocyte count, and improve immune response and oxidative resistance [5]. A deficiency in glutamine has been found to result in a decreased capacity of the immune system to withstand the impacts of chemotherapy, heightened permeability of the intestinal mucosa, potential bacterial translocation, and the initiation of a primary infection [6]. The exacerbation of diarrhea subsequent to oral administration of capecitabine may be attributable to this factor.

To date, examinations have demonstrated that tumors digest high quantities of glutamine as a vitality source. Cancer cells transport glutamine over the cytoplasmic film to frame glutamate at a quicker rate than their nonharmful partners [7]. Glutaminase, which catalyzes glutamine to glutamate, has been observed to be overexpressed in tumor cells [8]. In this way, our finding of diminished glutamine levels in serum is predictable, with the speculation that quickly developing tumor cells use glutamine from serum as an energy source. Glutamine is an essential amino acid able to impact tumor development [9–16] in the way that the amino acid glutamine is essential for the survival of stomach cancer cells [17]. Metabolomics proved to provide important information, especially in cancer genesis, being able to identify biomarkers for the early detection of cancer.

These days, chirality is crucial in a wide variety of industries, including the medical, pharmaceutical, and environmental sectors. Various illnesses have been linked to different enantiomers of the same chemical, suggesting that they may have distinct roles in the body and environment. Besides glycine (Gly), all of the other amino acids that may be used to make proteins also exhibit chirality. Despite the symmetry of D,L-amino acids, an enantiomeric pair, stereospecific biological processes precisely govern the stereostructures of amino acids, and the L-isomers of amino acids are the dominant form in natural systems. Accordingly, D-isomers are relatively insignificant enantiomers that were previously assumed to be completely functionally inert in biology.

Earlier, the group of Stefan-van Staden developed 3D stochastic sensors able to perform enantioanalysis of glutamine, demonstrating the correlation between DNA torsion and the emergence of D-glutamine in individuals afflicted with gastric carcinoma [18]. To avoid cross-contamination of samples from one patient to the other, it is necessary to develop a disposable enantioselective stochastic sensor able to perform the enantioanalysis of glutamine in biological samples such as gastric tumor tissue and whole blood. Therefore, this paper proposed an enantioselective disposable stochastic sensor, obtained by cold plasma deposition of graphene decorated with Ag on a plastic material. To obtain the stochastic signal, the material of the sensor was modified with maltodextrin having DE between 4.00 and 7.00. The advantage of this stochastic sensor versus the methods proposed to date for the analysis of glutamine that can be found in the literature (HPLC [19–23], flow injection analysis with potentiometric detection [24] and electrophoresis [25,26]), are: the stochastic sensor is able to perform enantioanalysis, no sampling is needed for the biological samples before measurements, the time of analysis is short (maximum 6 min), and analysis using stochastic sensors are cost-effective. Furthermore, the stochastic sensors

can perform qualitative and quantitative analysis [27,28]. The current development in stochastic sensors is based on the channel conductivity [27,28]: by entering the channel, the enantiomer is blocking it, and the current drops to zero (the time needed to enter is called  $t_{\text{off}}$ —the signature of the enantiomer); upon accessing the channel, redox reactions occur, whereby the duration of these reactions is referred to as  $t_{\text{on}}$ . The duration of  $t_{\text{on}}$  is contingent upon the concentration of the enantiomer present within the biological sample. Utilization of graphene as a matrix in the 2D stochastic sensors is made possible by the high stability of the channel needed for stochastic sensors; silver particles are added to improve the conductivity of the sensor, while the surface with maltodextrin is modified because maltodextrin possesses the potential to supply the required channels for stochastic sensing.

## 2. Materials and Methods

L- and D-glutamine, and maltodextrin (DE 4.00–7.00) were purchased from Sigma Aldrich. The glutamine solutions were prepared using phosphate buffer solution (PBS) with a pH of 7.50. The serial dilution method was employed to prepare L- and D-glutamine solutions ranging from  $10^{-3}$  to  $10^{-16}$  mol L<sup>-1</sup>.

Stochastic measurements were performed using a potentiostat/galvanostat EmStat Pico (PalmSens, Houten, The Netherlands) connected to a cellphone. All measurements were performed using a disposable 2D enantioselective stochastic sensor that consisted of the working sensor, a platinum site as the counter electrode, and the Ag/AgCl site as the reference electrode. Both graphene and silver nanocomposite layers were deposited on the plastic substrate by the cold plasma-coated method at room temperature, in high vacuum, from a special designed graphite anode, consisting of silver NPs (99.99%) and graphene (Nanoplatelets 99.90%) as target. The anode design allows the simultaneous deposition of graphene and Ag, and the plasma plume contains both material vapors and ions. The cold plasma method and the detailed deposition procedures have been described previously [29].

The design of the electrochemical sensor based on (a) the AgGR nanocomposite layer and AgNPs; (b) a digital photo of the coated and uncoated plastic substrate; and (c) flexibility of the sample is shown in Figure 1. It was designed based on the commercially available flexible plastic substrate (overhead projector transparency film suitable for use with photocopiers and laser printers) for the electrochemical sensor application. The flexibility of the sample after the coating process is shown in Figure 1c and the nanocomposite layer covers the plastic substrate.



**Figure 1.** The design of the electrochemical sensor is based on: (a) the AgGR nanocomposite layer and AgNPs, (b) a digital photo of the coated and uncoated plastic substrate, and (c) flexibility of the sample.

The morphology of the nanocomposite layer on a plastic substrate was characterized using a scanning electron microscope (SEM) at a magnification of  $2500\times$ . The samples were morphologically investigated at a voltage of 5 kV by secondary electrons, a current of 5 pA, and an applied pressure of  $1 \times 10^{-3}$  Pa. This voltage was used to avoid an electrostatic charge and to highlight the Ag particles. Moreover, the samples were also investigated elementarily with the help of an EDX detector at a voltage of 30 kV to highlight all the elements that appear on the sample (the same pressure of  $1 \times 10^{-3}$  Pa). The SEM top view image suggests the presence of AgNPs embedded in the AgGR nanocomposite layer, which

allows us to show elemental contrasts between carbon and silver (Figure 2a). The EDAX spectra presented in Figure 2b confirmed the existence of the proposed composition with some other elements in the plastic substrate, such as C, O, and Cl elements. The results of the EDAX elemental microanalysis of the nanocomposite layer are listed in Figure 2b.

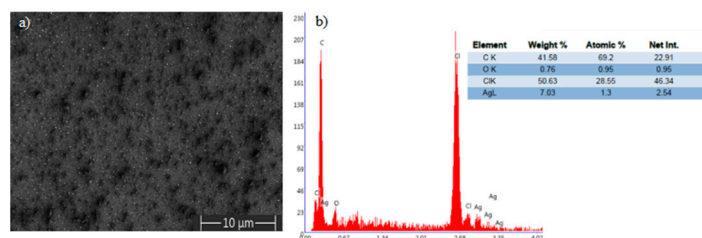
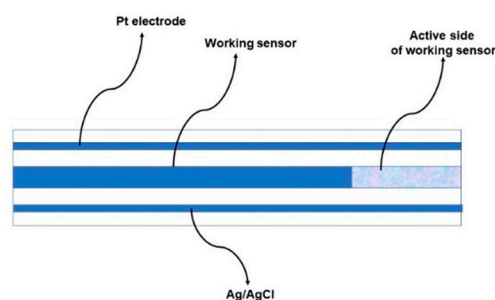


**Figure 2.** (a) Top-view scanning electron microscope images of deposited nanocomposite layer; (b) EDAX spectrum and elemental composition of deposition on plastic substrate.

Layers of Ag and AgCl as well as of Pt were deposited next to that of the working sensor to give the 2D enantioselective disposable stochastic sensor (Scheme 1). An addition consisting of a drop of maltodextrin (DE 4.00–7.00) solution (with a concentration of  $10^{-3}$  mol L $^{-1}$ ) was cast to the active side of the working sensor, and it was left to dry for 24 h before utilization. Due to the porous structure of the electrode surface (Figure 2a), the maltodextrin solution was well adsorbed into the surface.



**Scheme 1.** 2D Enantioselective Disposable Stochastic Sensor.

### 2.1. Stochastic Mode

All measurements were performed at a constant 25 degrees Celsius.  $t_{on}$  and  $t_{off}$  were measured using a constant potential chronoamperometric technique (174 mV vs. Ag/AgCl). L- or D-glutamine was added to the single-use sensor at a concentration between  $10^{-16}$  and  $10^{-3}$  mol L $^{-1}$ . Calibration equations for L- and D-glutamine were found by the linear regression method. The  $t_{off}$  values shown in Figure 3 were used to determine the two enantiomers.

The concentrations of L and D glutamine, which were previously unknown, were ascertained through the utilization of calibration equations and the corresponding  $t_{on}$  values that were identified for each enantiomer in the diagrams.

### 2.2. Samples

Blood samples were collected from confirmed gastric cancer patients who were not undergoing any treatment, as well as from healthy individuals who served as negative controls. The samples were obtained from the County Emergency Hospital in Targu-Mures. The aforementioned samples were obtained from individuals who were diagnosed with gastric cancer and those who were deemed healthy volunteers. The collection of these specimens was carried out in accordance with the protocols outlined in the Ethics committee approval number 32647/2018, which was granted by the County Emergency Hospital in Targu-Mures. All patients provided informed consent. No pretreatment was necessary for the analysis of the samples. Whole blood droplets or gastric tumor tissue samples were

applied onto the disposable sample, and the stochastic mode as previously described was utilized to determine the concentrations of the biomarkers of unknown quantities.

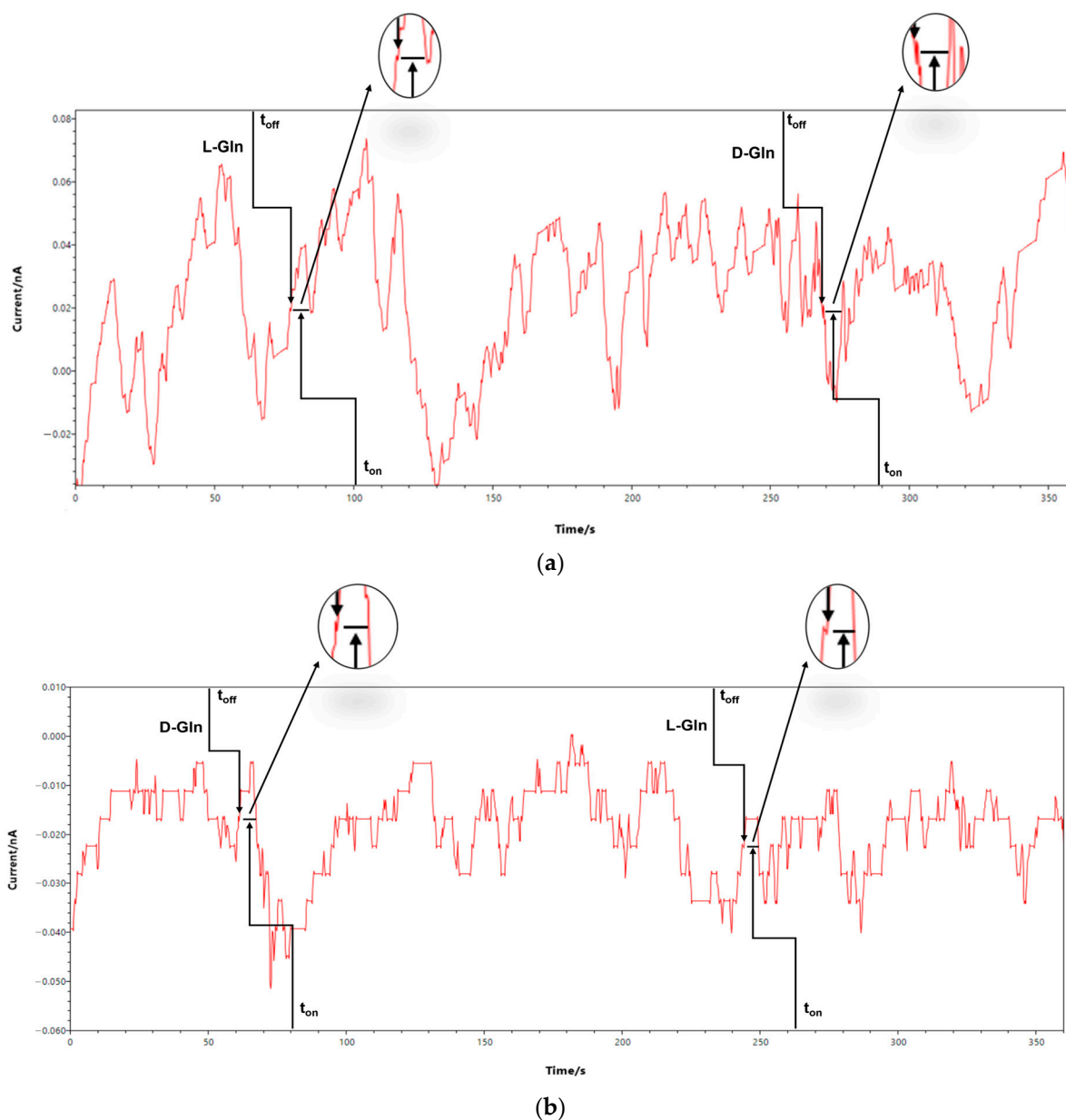


**Figure 3.** Examples of diagrams obtained for the enantioanalysis of glutamine using 2D enantioselective stochastic sensors from (a) whole blood and (b) tissue sample.

### 3. Results

#### 3.1. Response Characteristics of the 2D Enantioselective Stochastic Sensors

Chronoamperometry was utilized for all measurements, with a constant potential of 174 mV vs. Ag/AgCl. Upon application of the potential, the enantiomers migrated towards the electrode interface and subsequently entered the channel. During the entry process, the current intensity was observed to be zero. The duration of this entry process is referred to as the enantiomer's signature, denoted as  $t_{off}$  in the accompanying diagrams. During their presence in the channel, the enantiomers experience binding and redox phenomena. The duration required for these processes to occur is denoted as " $t_{on}$ " on the diagram, and it falls within the range of two " $t_{off}$ " values. For the assay of L-glutamine, the following response characteristics were obtained when calibration was done in clean

buffer solutions: signature of L-glutamine ( $t_{\text{off}}$  value)  $1.4 \pm 0.1$  s, linear concentration range of  $1 \times 10^{-13}$ – $1 \times 10^{-3}$  mol L<sup>-1</sup>, limit of quantification  $1 \times 10^{-13}$  mol L<sup>-1</sup>, sensitivity of  $1.72 \times 10^{10}$  s<sup>-1</sup> mol<sup>-1</sup> L, and the equation of calibration:

$$\frac{1}{t_{\text{on}}} = 0.28 + 1.72 \times 10^{10}C \quad (1)$$

( $\langle t_{\text{on}} \rangle = \text{s}$ ;  $\langle C \rangle = \text{mol L}^{-1}$ ) where  $r = 0.9996$ . When the calibration was repeated in the whole blood from a healthy volunteer, the calibration graph was:

$$\frac{1}{t_{\text{on}}} = 0.30 + 1.74 \times 10^{10}C \quad (2)$$

( $\langle t_{\text{on}} \rangle = \text{s}$ ;  $\langle C \rangle = \text{mol L}^{-1}$ ) where  $r = 0.9999$  and a sensitivity of  $1.74 \times 10^{10}$  s<sup>-1</sup> mol<sup>-1</sup> L. The linear concentration range and the limit of quantification did not change when using whole blood for calibration.

For the assay of D-glutamine, the following response characteristics were obtained when calibration was done in clean buffer solutions: signature of D-glutamine ( $t_{\text{off}}$  value)  $0.3 \pm 0.1$  s, linear concentration range of  $1 \times 10^{-15}$ – $1 \times 10^{-3}$  mol L<sup>-1</sup>, limit of quantification  $1 \times 10^{-15}$  mol L<sup>-1</sup>, sensitivity of  $1.17 \times 10^{13}$  s<sup>-1</sup> mol<sup>-1</sup> L, and the equation of calibration:

$$\frac{1}{t_{\text{on}}} = 0.26 + 1.17 \times 10^{13}C \quad (3)$$

( $\langle t_{\text{on}} \rangle = \text{s}$ ;  $\langle C \rangle = \text{mol L}^{-1}$ ) where  $r = 0.9998$ . When the calibration was repeated in the whole blood from a healthy volunteer, the calibration graph was:

$$\frac{1}{t_{\text{on}}} = 0.20 + 1.20 \times 10^{13}C \quad (4)$$

( $\langle t_{\text{on}} \rangle = \text{s}$ ;  $\langle C \rangle = \text{mol L}^{-1}$ ) where  $r = 0.9999$  and a sensitivity of  $1.20 \times 10^{13}$  s<sup>-1</sup> mol<sup>-1</sup> L. The linear concentration range and the limit of quantification did not change, when using whole blood for calibration.

Slight differences were observed between the sensitivities recorded when biological samples were used, while no differences were recorded regarding limits of determination and working concentration ranges.

The variances observed in the signatures' values provided evidence of the sensor's enantioselectivity, the two enantiomers being able to be determined simultaneously in the biological samples. High sensitivity values were recorded, with low limits of determination, making possible their assay in healthy people as well as in patients with gastric cancers in different stages.

Reproducibility studies were conducted in the following manner: ten sensors were produced in accordance with the methodology outlined in the Sensor Design section. The evaluation process for each sensor was standardized, and the respective sensitivities were ascertained and juxtaposed while being submerged in solutions of L-glutamine and D-glutamine. The recorded RSD (%) values for the sensitivities were 0.10% for the L-glutamine assay and 0.11% for the D-glutamine assay. The recorded RSD (%) values, referring to the sensitivities, have demonstrated the reproducibility of the design of the sensors.

The stability of individual 2D sensors, which were intended for single use, was assessed in the following manner: a total of 10 sensors of each type were subjected to storage conditions as outlined in the Sensors Design section. On a daily basis, a distinct sensor was retrieved from storage and subjected to immersion in solutions containing varying concentrations of L- and D-glutamine. The sensitivity of each measurement was recorded and retained for comparative purposes after the entire batch of sensors had been utilized over a period of 30 days. The findings obtained at the conclusion of the timeframe

indicate that the electrodes exhibited a notable level of stability over time, as evidenced by the sensitivities' temporal variations being less than 0.50%.

### 3.2. The Selectivity and Enantioselectivity of the 2D Stochastic Sensors

The determination of selectivity and enantioselectivity is based on the identification of enantiomers and analytes present in real samples. The presence of dissimilar values in the signatures indicates that the sensor under consideration is both enantioselective and selective. The signatures of the analytes were found to be independent of the matrix from which they were derived. However, they were observed to be influenced by factors such as the stereochemistry of the enantiomers, the length and volume of the molecules, and their velocity of movement within the channel. The analytes present in a solution are observed to enter the channel in a specific sequence, which is determined by the length and stereochemistry of the molecules. The enantioselectivity of a 2D sensor was demonstrated by recording distinct  $t_{\text{off}}$  values for L- and D-glutamine, as shown in Table 1. To evaluate selectivity, additional amino acids, namely tryptophan (Trp), proline (Pro), and arginine (Arg), were chosen. Distinctive signatures were acquired for the aforementioned amino acids in contrast to the signatures documented for L- and D-glutamine, thereby validating the selectivity of the 2D sensors (refer to Table 1).

**Table 1.** Selectivity of the 2D disposable stochastic sensors (N = 10).

| Interferent | Signature, $t_{\text{off}}$ (s) |           |           |           |           |           |           |           |
|-------------|---------------------------------|-----------|-----------|-----------|-----------|-----------|-----------|-----------|
|             | L-gln                           | D-gln     | L-try     | D-try     | L-pro     | D-pro     | L-arg     | D-arg     |
| -           | 0.7 ± 0.1                       | 1.9 ± 0.1 | 2.2 ± 0.1 | 1.2 ± 0.1 | 2.0 ± 0.1 | 2.5 ± 0.1 | 3.1 ± 0.1 | 3.5 ± 0.1 |

The reliability of the recorded values for the signatures is contingent upon the size and geometry of the amino acid that was tested.

## 4. Discussion

### *Enantioanalysis of Glutamine in Whole Blood and Tumor Tissue Samples*

Research efforts are heavily focused on improving analytical procedures for analyzing amino acids because of their enormous nutritional, biotechnological, and therapeutic value. These new analyses are particularly suited to electrochemical approaches. Electrochemical sensing techniques are intriguing alternatives to conventional clinical approaches because they allow for the straightforward, rapid, low-cost, sensitive, and, to some degree, selective detection of bioanalytes important to clinical diagnostic testing. Electrochemical techniques can be employed as efficient sensing procedures due to the large range of approaches that have been developed for signal transduction and target identification. Therefore, electrochemical sensing systems, which rely heavily on bioaffinity identification and electrochemical transduction techniques, are making the transition from the realm of laboratory research to the point-of-care detection of biomolecules like lactate, glucose, and glutamine.

Electrochemical techniques have several advantages; however, distinguishing between d-amino acids and their L-isomer is difficult due to the similarity of their electrochemical signals. For electroactive amino acids, signal overlapping and/or significant overpotential continue to be a major obstacle. However, with the help of stochastic sensing, this concern can be overcome due to the fact that these types of sensors can identify the L- or D- isomer of an amino acid through the unique signature of each biomarker.

Whole blood and tissue samples were collected from individuals diagnosed with gastric cancer. Healthy individuals were recruited to provide whole blood samples. The biological specimens were examined in their original state, utilizing the stochastic approach outlined previously.

The precision of the screening examinations utilizing the 2D enantioselective stochastic sensors was demonstrated via the standard addition of L- and D-glutamine to the biological specimens. Recovery tests were conducted on samples containing L-glutamine and D-

glutamine using the following procedure: L- and D-glutamine were first identified in the samples, followed by the addition of predetermined quantities of L- and D-glutamine. The quantities of L- and D-glutamine that were retrieved were juxtaposed with those that were introduced into the entirety of the blood specimen.

The results presented in Table 2 demonstrate that the proposed 2D stochastic sensors can accurately detect L- and D-glutamine in whole blood samples. The recovery of the individual is not impacted by the proportion of L- and D-enantiomers present in glutamine.

**Table 2.** Recovery tests of L- and D-glutamine in whole blood samples (N = 10).

| L:D | Recovery%       |                 |                 |                 |                 |                 |                 |                 |                 |                 |                 |                 |                 |                 |
|-----|-----------------|-----------------|-----------------|-----------------|-----------------|-----------------|-----------------|-----------------|-----------------|-----------------|-----------------|-----------------|-----------------|-----------------|
|     | 1:99            |                 | 1:50            |                 | 1:25            |                 | 1:1             |                 | 25:1            |                 | 50:1            |                 | 99:1            |                 |
|     | Enantiomer      | L               | D               | L               | D               | L               | D               | L               | D               | L               | D               | L               | D               | L               |
|     | 99.15<br>± 0.02 | 99.35<br>± 0.03 | 99.47<br>± 0.04 | 99.12<br>± 0.04 | 99.90<br>± 0.05 | 99.21<br>± 0.05 | 99.98<br>± 0.07 | 99.97<br>± 0.05 | 99.87<br>± 0.05 | 99.12<br>± 0.06 | 99.88<br>± 0.08 | 99.78<br>± 0.06 | 99.95<br>± 0.05 | 99.93<br>± 0.03 |

Table 3 shows the results obtained for 10 whole blood samples and 10 gastric tumor tissue samples. The samples were screened accordingly with the stochastic method described above using the 2D enantioselective stochastic sensor. The identification of L-glutamate and D-glutamate in the samples was based on their respective signatures,  $t_{off}$  values, as illustrated in Figure 3. The enantiomeric concentrations of glutamine were ascertained by employing the respective calibration equations for each enantiomer. The  $t_{on}$  values, which were obtained by measuring between two consecutive  $t_{off}$  values as depicted in Figure 3, were utilized for this purpose. The study findings indicate the presence of L- and D-glutamine in the entirety of blood and gastric tumor tissues of the patients who were diagnosed with gastric cancer, as presented in Table 3.

**Table 3.** Enantioanalysis of glutamine in whole blood and gastric tumor tissue samples of confirmed patients with gastric cancer.

| Sample No. | Enantiomer of Glutamine | Glutamine ( $\mu\text{mol}^{-1}$ ) <sup>1</sup> | Enantiomeric Excess (%) |
|------------|-------------------------|---|-------------------------|
|            |                         | Whole blood                                     |                         |
| 1          | L                       | 2.04 ± 0.03                                     | 61.26                   |
|            | D                       | 0.49 ± 0.02                                     |                         |
| 2          | L                       | 5.84 ± 0.04                                     | 89.33                   |
|            | D                       | $3.29 (\pm 0.02) \times 10^{-1}$                |                         |
| 3          | L                       | 2.13 ± 0.02                                     | 58.07                   |
|            | D                       | $5.65 (\pm 0.03) \times 10^{-1}$                |                         |
| 4          | L                       | 1.76 ± 0.02                                     | 34.04                   |
|            | D                       | $8.66 (\pm 0.02) \times 10^{-1}$                |                         |
| 5          | L                       | 2.35 ± 0.03                                     | 99.73                   |
|            | D                       | $3.22 (\pm 0.01) \times 10^{-3}$                |                         |
| 6          | L                       | 2.26 ± 0.03                                     | 62.01                   |
|            | D                       | 0.53 ± 0.03                                     |                         |
| 7          | L                       | 1.06 ± 0.01                                     | 92.17                   |
|            | D                       | $4.32 (\pm 0.03) \times 10^{-2}$                |                         |
| 8          | L                       | 4.37 ± 0.04                                     | 90.79                   |
|            | D                       | $2.11 (\pm 0.02) \times 10^{-1}$                |                         |
| 9          | L                       | 1.05 ± 0.01                                     | 95.28                   |
|            | D                       | $2.54 (\pm 0.02) \times 10^{-2}$                |                         |
| 10         | L                       | 5.84 ± 0.03                                     | 91.70                   |
|            | D                       | $2.53 (\pm 0.01) \times 10^{-1}$                |                         |

Table 3. Cont.

| Sample No.           | Enantiomer of Glutamine | Glutamine ( $\mu\text{mol}^{-1}$ ) <sup>1</sup> | Enantiomeric Excess (%) |
|----------------------|-------------------------|---|-------------------------|
| Gastric tumor tissue |                         |   |                         |
| 1                    | L                       | $1.05 \pm 0.01$                                 | 56.72                   |
|                      | D                       | $0.29 \pm 0.02$                                 |                         |
| 2                    | L                       | $1.33 \pm 0.03$                                 | 69.32                   |
|                      | D                       | $2.41 (\pm 0.02) \times 10^{-1}$                |                         |
| 3                    | L                       | $1.66 \pm 0.02$                                 | 86.83                   |
|                      | D                       | $1.17 (\pm 0.03) \times 10^{-1}$                |                         |
| 4                    | L                       | $5.83 \pm 0.02$                                 | 64.69                   |
|                      | D                       | $1.25 \pm 0.03$                                 |                         |
| 5                    | L                       | $2.04 \pm 0.04$                                 | 88.37                   |
|                      | D                       | $1.26 (\pm 0.02) \times 10^{-1}$                |                         |
| 6                    | L                       | $1.06 \pm 0.02$                                 | 3.64                    |
|                      | D                       | $1.14 \pm 0.03$                                 |                         |
| 7                    | L                       | $1.33 \pm 0.02$                                 | 59.47                   |
|                      | D                       | $3.38 (\pm 0.03) \times 10^{-1}$                |                         |
| 8                    | L                       | $3.75 \pm 0.03$                                 | 92.21                   |
|                      | D                       | $1.52 (\pm 0.02) \times 10^{-1}$                |                         |
| 9                    | L                       | $1.06 \pm 0.03$                                 | 3.41                    |
|                      | D                       | $0.99 \pm 0.02$                                 |                         |
| 10                   | L                       | $7.51 \pm 0.02$                                 | 95.62                   |
|                      | D                       | $1.68 (\pm 0.03) \times 10$                     |                         |

<sup>1</sup> All results are the average of 5 measurements.

The stochastic sensors were utilized to analyze whole blood samples obtained from healthy individuals. The enantioanalysis results indicated that solely the L-enantiomer of glutamine was present in the healthy patients, with no detection of D-glutamine in their whole blood (as presented in Table 4). Further, the enantiomeric excess may be a trademark of the evolution of illness.

Table 4. Enantioanalysis of glutamine in whole blood samples of healthy volunteers.

| Sample No. | Enantiomer of Glutamine | L-Glutamine, $\text{mmol L}^{-1}$ |
|------------|-------------------------|-----------------------------------|
| 1          | L                       | $0.46 \pm 0.02$                   |
| 2          | L                       | $0.30 \pm 0.02$                   |
| 3          | L                       | $0.26 \pm 0.01$                   |
| 4          | L                       | $0.13 \pm 0.02$                   |
| 5          | L                       | $0.11 \pm 0.01$                   |

Compared with the results obtained by Meyerhoff et al. [24] using a biosensor for the assay of L-glutamine as detector in flow injection analysis, the proposed 2D enantioselective stochastic sensor can be designed more easily than the biosensor, no special storage conditions are required for the stochastic sensor compared with the biosensor that must be kept at 4 °C, the biosensor had very low stability in time, and the linear concentration range is wider for the stochastic sensor compared with the biosensor ( $1 \times 10^{-4}$ – $1 \times 10^{-2}$  mol L<sup>-1</sup>), with a higher limit of determination for the biosensor compared with the stochastic sensor. The biosensor can only determine the L-glutamine, while the stochastic sensor can determine, in the same run, both enantiomers of glutamine.

## 5. Conclusions

Stereospecific biological mechanisms accurately determine the stereostructures of amino acids, and the L-isomers of amino acids are the dominant form in natural systems despite the symmetry of the D,L-amino acid pair. D-enantiomers have long been known for not having any biological function. To explore the potential roles of D-amino acids, a novel approach for simultaneous analysis of D,L-amino acids in biological materials

is required. A 2D enantioselective disposable stochastic sensor was proposed for the enantioanalysis of glutamine in whole blood and gastric tumor tissue samples. The high sensitivity of the sensor as well as its wide working concentration range made possible the analysis of samples from confirmed patients with gastric cancer, as well as from healthy volunteers. The main feature is its utilization for fast screening tests for the early detection of gastric cancer, based on the identification of D-glutamine, the quantification of L- and D-glutamine, and the determination of enantiomeric excess, especially given that the sensors were connected to a mobile device able to record and read the diagrams.

**Author Contributions:** Conceptualization, R.-I.S.-v.S.; methodology, R.-I.S.-v.S., R.-M.I.-M. and D.-C.G.; validation, M.I.B., R.-M.I.-M., D.-C.G. and R.-I.S.-v.S.; formal analysis, R.-I.S.-v.S.; investigation, M.I.B., R.-M.I.-M., M.B. and D.-C.G.; writing—original draft preparation, R.-I.S.-v.S., M.I.B. and M.B.; writing—review and editing, R.-I.S.-v.S., R.-M.I.-M. and D.-C.G.; supervision, R.-I.S.-v.S.; project administration, R.-I.S.-v.S.; funding acquisition, R.-I.S.-v.S. All authors have read and agreed to the published version of the manuscript.

**Funding:** This work was supported by Nucleus Program within the framework of the National Plan for Research, Development and Innovation 2022–2027, carried out with the support of the Ministry of Research, Innovation and Digitization, project number PN 23 27 03 01.

**Informed Consent Statement:** Informed consent was obtained from all patients.

**Data Availability Statement:** Data is unavailable due to ethical restrictions.

**Acknowledgments:** This work was supported by Nucleus Program within the framework of the National Plan for Research, Development and Innovation 2022–2027, carried out with the support of the Ministry of Research, Innovation and Digitization, project number PN 23 27 03 01.

**Conflicts of Interest:** The authors declare that they have no conflict of interest.

**Ethical Statement:** The study was conducted in accordance with the Declaration of Helsinki, and the protocol was approved by the Ethics Committee of County Emergency Hospital from Targu-Mures 32647/2018 (Project identification code: PN-III-P4-ID-PCCF-0006). All subjects gave their informed consent for inclusion before they participated in the study.

## References

1. Eagle, H.; Oyama, V.I.; Levy, M.; Horton, C.L.; Fleischman, R. The growth response of mammalian cells in tissue culture to l-glutamine and l-glutamic acid. *J. Biol. Chem.* **1956**, *218*, 607–616. [[CrossRef](#)] [[PubMed](#)]
2. Altman, B.J.; Stine, Z.E.; Dang, C.V. From krebs to clinic: Glutamine metabolism to cancer therapy. *Nat. Rev. Cancer* **2016**, *16*, 619–634. [[CrossRef](#)]
3. Curthoys, N.P.; Watford, M. Regulation of glutaminase activity and glutamine metabolism. *Annu. Rev. Nutr.* **1995**, *15*, 133–159. [[CrossRef](#)]
4. Wise, D.R.; Thompson, C.B. Glutamine addiction: A new therapeutic target in cancer. *Trends Biochem. Sci.* **2010**, *35*, 427–433. [[CrossRef](#)] [[PubMed](#)]
5. Hu, K.; Zhang, J.X.; Feng, L.; Jiang, W.D.; Wu, P.; Liu, Y.; Jiang, J.; Zhou, X.Q. Effect of dietary glutamine on growth performance, non-specific immunity, expression of cytokine genes, phosphorylation of target of rapamycin (TOR), and anti-oxidative system in spleen and head kidney of Jian carp (*Cyprinus carpio* var. Jian). *Fish. Physiol. Biochem.* **2015**, *41*, 635–649. [[CrossRef](#)] [[PubMed](#)]
6. Pujos-Guillot, E.; Pickering, G.; Lyan, B.; Ducheix, G.; Brandolini-Bunlon, M.; Glomot, F.; Dardevet, D.; Dubray, C.; Papet, I. Therapeutic paracetamol treatment in older persons induces dietary and metabolic modifications related to sulfur amino acids. *Age* **2012**, *34*, 181–193. [[CrossRef](#)]
7. Medina, M.A. Glutamine and cancer. *J. Nutr.* **2001**, *131*, 2539S–2542S. [[CrossRef](#)]
8. DeBerardinis, R.J.; Lum, J.J.; Hatzivassiliou, G.; Thompson, C.B. The biology of cancer: Metabolic reprogramming fuels cell growth and proliferation. *Cell Metab.* **2008**, *7*, 11–20. [[CrossRef](#)]
9. Sauer, L.A.; Stayman, J.W.; Dauchy, R.T. Amino acid, glucose, and lactic acid utilization in vivo by rat tumors. *Cancer Res.* **1982**, *42*, 4090–4097.
10. Kovacevic, Z.; Morris, H.P. The role of glutamine in the oxidative metabolism of malignant cells. *Cancer Res.* **1972**, *32*, 326–333.
11. Miller, T.J.; Franco, R.S.; Chance, W.T.; Orlando, J.; Martelo, M.D.; Popp, M.B. Amino acid requirements of rat sarcoma as determined by a stem cell assay. *J. Parenter. Enter. Nutr.* **1987**, *11*, 223–228. [[CrossRef](#)] [[PubMed](#)]
12. Frisell, W.R. Synthesis and catabolism of nucleotides. In *Human Biochemistry*; Frisell, W.R., Ed.; MacMillan: New York, NY, USA, 1982; p. 292.

13. Knox, W.E.; Horowitz, M.L.; Friedell, G.H. The proportionality of glutaminase content to growth rate and morphology of rat neoplasms. *Cancer Res.* **1969**, *29*, 669–680.
14. Souba, W.W.; Strebel, F.R.; Bull, J.M.; Copeland, E.M.; Teagtmeyer, H.; Cleary, K. Interorgan glutamine metabolism in the tumor-bearing rat. *J. Surg. Res.* **1988**, *44*, 720–726. [[CrossRef](#)]
15. Popp, M.B.; Enrione, E.B.; Wagner, S.C.; Chance, W.T. Influence of total nitrogen, asparagines and glutamine on MCA tumor growth in the Fischer 344 rat. *Surgery* **1998**, *104*, 152–160.
16. Chance, W.T.; Cao, L.; Nelson, J.L.; Kim, M.W.; Fischer, J.E. Reduction of tumor growth following treatment with glutamine antimetabolite. *Life Sci.* **1988**, *42*, 87–94. [[CrossRef](#)]
17. Xio, S.; Zhou, L. Gastric cancer: Metabolic and metabolomics perspectives. *Int. J. Oncol.* **2017**, *51*, 5–17. [[CrossRef](#)] [[PubMed](#)]
18. Stefan-van Staden, R.I.; Ilie-Mihai, R.M.; Magerusan, L.; Coros, M.; Pruneanu, S. Enantioanalysis of glutamine—A key factor in establishing the metabolomics process in gastric cancer. *Anal. Bioanal. Chem.* **2020**, *412*, 3199–3207. [[CrossRef](#)]
19. Polanuer, B.; Sholin, A.; Demina, N.; Rumiantseva, N. Determination of glutamine, glutamic acid and pyroglutamic acids using high-performance liquid chromatography on dynamically modified silica. *J. Chromatogr. A* **1992**, *594*, 173–178. [[CrossRef](#)]
20. Monge-Acuña, A.A.; Fornaguera-Trías, J. A high performance liquid chromatography method with electrochemical detection of gamma-aminobutyric acid, glutamate and glutamine in rat brain homogenates. *J. Neurosci. Methods* **2009**, *183*, 176–181. [[CrossRef](#)]
21. Tcherkas, Y.V.; Kartsova, L.A.; Krasnova, I.N. Analysis of amino acids in human serum by isocratic reversed-phase high-performance liquid chromatography with electrochemical detection. *J. Chromatogr. A* **2001**, *913*, 303–308. [[CrossRef](#)] [[PubMed](#)]
22. Han, M.; Xie, M.; Han, J.; Yuan, D.; Yang, T.; Xie, Y. Development and validation of a rapid, selective, and sensitive LC–MS/MS method for simultaneous determination of d- and l-amino acids in human serum: Application to the study of hepatocellular carcinoma. *Anal. Bioanal. Chem.* **2018**, *410*, 2517–2531. [[CrossRef](#)] [[PubMed](#)]
23. Raimbault, A.; Dorebska, M.; West, C. A chiral unified chromatography–mass spectrometry method to analyze free amino acids. *Anal. Bioanal. Chem.* **2019**, *411*, 4909–4917. [[CrossRef](#)]
24. Meyerhoff, M.E.; Trojanowicz, M.; Palsson, B.O. Simultaneous enzymatic/electrochemical determination of glucose and L-glutamine in hybridoma media by flow-injection analysis. *Biotechnol. Bioeng.* **1993**, *41*, 964–969. [[CrossRef](#)]
25. Prior, A.; Coliva, G.; de Jong, G.J.; Somsen, G.W. Chiral capillary electrophoresis with UV-excited fluorescence detection for the enantioselective analysis of 9-fluorenylmethoxycarbonyl-derivatized amino acids. *Anal. Bioanal. Chem.* **2018**, *410*, 4979–4990. [[CrossRef](#)]
26. Stefan-van Staden, R.I.; Comnea-Stancu, I.R.; Yanik, H.; Göksel, M.; Alexandru, A.; Durmuş, M. Phthalocyanine-BODIPY dye: Synthesis, characterization, and utilization for pattern recognition of CYFRA 21-1 in whole blood samples. *Anal. Bioanal. Chem.* **2017**, *409*, 6195–6203. [[CrossRef](#)] [[PubMed](#)]
27. Stefan-van Staden, R.I.; Comnea-Stancu, I.R.; Surdu-Bob, C.C. Molecular screening of blood samples for the simultaneous detection of CEA, HER-1, NSE, CYFRA 21-1 using stochastic sensors. *J. Electrochem. Soc.* **2017**, *164*, B267–B273. [[CrossRef](#)]
28. Stefan-van Staden, R.I.; Moscalu-Lungu, A.; Badulescu, M. Disposable Stochastic Sensors Based on Nanolayer Deposition(s) of Silver and AgC Composite on Plastic for the Assay of alpha-amylase in Whole Blood and Saliva. *Nanomaterials* **2020**, *10*, 1528. [[CrossRef](#)]
29. Gheorghe, S.S.; Cioates Negut, C.; Badulescu, M.; Stefan-van Staden, R.I. Sensitive Detection of Heregulin- $\alpha$  from Biological Samples Using a Disposable Stochastic Sensor Based on Plasma Deposition of GNPs-AgPs' Nanofilms on Silk. *Life* **2021**, *11*, 894. [[CrossRef](#)]

**Disclaimer/Publisher's Note:** The statements, opinions and data contained in all publications are solely those of the individual author(s) and contributor(s) and not of MDPI and/or the editor(s). MDPI and/or the editor(s) disclaim responsibility for any injury to people or property resulting from any ideas, methods, instructions or products referred to in the content.